Int. J. Multiphase Flow, Vol. 2, pp. 581–589. Pergamon/Elsevier, 1976. Printed in Great Britain.

BOUNDS ON THE DRAG FOR CREEPING FLOW OF AN ELLIS FLUID PAST AN ASSEMBLAGE OF SPHERES

V. MOHAN† and J. RAGHURAMAN‡

Department of Chemical Engineering, Indian Institute of Technology, Madras 600036, India

(*Received* 29 *August* 1974)

Abstract—Upper and lower bounds for the creeping flow of an Ellis fluid past an assemblage of solid spheres are obtained using a combination of Happel's free surface model and variational principles. The arithmetic mean of the bounds agrees closely with the experimental data on flow through porous media. For Ellis numbers approaching infinity, the analysis also predicts the bounds for a power law fluid.

1. INTRODUCTION

Fluid–particle systems with large volume fraction of solids are encountered in flow through porous media and in fluidized beds. Several attempts have been made to model these systems, the most popular of which are the free surface cell model of Happel (1958) and the zero vorticity model of Kuwabara (1959). In these models, wall effects and end effects are neglected and the assembly of particles are assumed to be uniformly spaced in the fluid. The interaction of a particle with the neighbouring ones is modelled by assuming the particle to be surrounded by a hypothetical spherical envelope whose radius is related to the voidage of the multiparticle assemblage. Each sphere with its spherical envelope is uncoupled from the system and treated separately. The particle interaction and the voidage are imposed on the cell by the position of the outer spherical boundary with respect to the sphere diameter and the mathematical boundary conditions placed on the surface. The free surface model of Happel imposes a zero shear stress and zero radial velocity on the hypothetical surface while the model due to Kuwabara imposes a condition of zero vorticity. Therefore it is quite clear that in the Happel's model, no force would exist on the hypothetical fluid surface except in the direction of the normal. Furthermore, since the radial velocity on the hypothetical fluid surface is zero, the cell does no work on the surroundings. On the other hand, the latter model is in conceptual error, for, the unit cell does work on the surroundings (Happel & Brenner 1965). The free surface model enables prediction of pressure drop and hindered settling in concentrated systems of spheres (Happel & Brenner 1965) and the drag in packed and fluidized beds remarkably well in the range of porosities $0.3 \leq \epsilon \leq 0.6$. Using the above cell models, the flow of a Newtonian fluid past an assemblage of solid spheres was analysed by Happel (1958) for creeping flow and by Le Clair & Hamielec (1968) and El-Kaissy & Homsy (1973) for intermediate Reynolds number flows.

The flow of non-Newtonian fluids through porous media is encountered in polymer processing operations, recovery of underground oil etc., and many experimental studies (Savins 1969) have been reported treating the polymer melt or aqueous polymer solutions as power law fluids. The flow of a power law non-Newtonian fluid past a single sphere has been studied by a number of investigators (Tomita 1959; Wallick, Savins & Arterburn 1962; Slattery 1962; Wasserman & Slattery 1964; Adachi, Yoshioka & Yamamoto 1973). However, despite the fact that the Ellis model is superior to the power law model in that it predicts a finite viscosity at zero shear rate, the flow of a non-Newtonian Ellis fluid past solid spheres has not been analysed in detail. The creeping flow of an Ellis fluid past single solid and fluid spheres was analysed theoretically by Hopke and Slattery (1970) and Mohan and Venkateswarlu (1974) respectively. Sadowski and Bird (1965) and Sadowski (1965) studied the flow of an Ellis fluid in a packed bed using aqueous solutions of polyethylene glycol, polyvinyl alcohol and natrosol. A capillary approach was used

†Present address: Department of Chemical Engineering, Illinois Institute of Technology, Chicago, IL 60616, U.S.A.
‡Present address: Department of Chemical Engineering, Monash University, Clayton, Victoria, 3168, Australia.

by them for correlating the pressure drop data. In the present work, the bounds on the drag coefficient are obtained for the creeping flow of an Ellis fluid past an assemblage of solid spheres using a combination of Happel's free surface model and the variational principles due to Slattery (1972). The results are compared with the experimental data of Sadowski (1965).

2. STATEMENT OF THE PROBLEM

Consider the steady, incompressible, creeping flow of an Ellis fluid past an assemblage of insoluble solid spheres of radius a (figure 1). The internal sphere moves in the direction of the positive Z-axis with a velocity V_0 (equal to the superficial velocity of the fluid in the assemblage) inside a hypothetical spherical fluid envelope of radius R_∞, on which the radial velocity and tangential stress are zero. The equation of continuity and the equation of motion for the flow situation are:

$$\nabla \cdot \mathbf{v} = 0, \quad [1]$$

$$-\nabla p + \nabla \cdot \boldsymbol{\tau} + \rho \mathbf{f} = 0, \quad [2]$$

where $\mathbf{v}$ is the velocity vector, $\boldsymbol{\tau}$ is the extra stress tensor, p is the pressure, ρ is the density of the fluid, and $\mathbf{f}$ is the body force.

In the spherical polar co-ordinate system (R, θ, ϕ), the boundary conditions on the surface of the sphere are given by

At $$r = 1,\ v_r = V_0 z,$$
$$v_\theta = -V_0(1 - z^2)^{1/2}, \quad [3a,b]$$

where $z = \cos\theta$ and $r = R/a$.

The boundary conditions on the free surface are

At $$r = r_\infty,\ v_r = 0,$$
$$\tau_{r\theta} = 0 \quad \text{or} \quad \frac{\partial}{\partial r}\left(\frac{v_\theta}{r}\right) = 0, \quad [4a,b]$$

where r_∞ is the dimensionless radius of the cell related to the voidage in the assemblage by the relation

$$r_\infty = R_\infty/a = (1 - \epsilon)^{-1/3}. \quad [5]$$

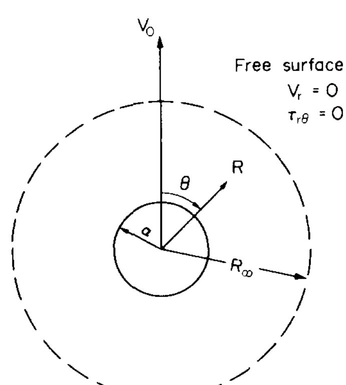

Figure 1. Schematic diagram of the flow system.

Analysis

For the steady creeping flow of an incompressible fluid, two variational principles were given by Slattery (1972). In what follows, we use the notations V, $\mathbf{T}$, $\mathbf{I}$, $\mathbf{n}$ and $\bar{\phi}$ to represent the flow domain, the stress tensor, the unit tensor, the normal on the bounding surface S and the body force potential respectively.

The velocity variational principle:

$$\int_V E\,\mathrm{d}V \leqslant \int_V E^*\,\mathrm{d}V - \int_{S-S_v} (\mathbf{v}^* - \mathbf{v}) \cdot ([\mathbf{T} - \rho\bar{\phi}I] \cdot \mathbf{n})\,\mathrm{d}S. \qquad [6]$$

The quantities with superscript asterisk are evaluated on the basis of a trial velocity profile that satisfies the equation of continuity and prescribed conditions for velocity on S_v, where S_v is that part of the bounding surface on which the velocity is explicitly specified.

The stress variational principle:

$$\int_V E\,\mathrm{d}V \geqslant -\int_V E_c^*\,\mathrm{d}V + \int_S \mathbf{v} \cdot ([\mathbf{T}^* - \rho\bar{\phi}\mathbf{I}] \cdot \mathbf{n})\,\mathrm{d}S. \qquad [7]$$

The quantities with a superscript asterisk are evaluated on the basis of a trial extra stress profile that satisfies Cauchy's first law and the prescribed conditions for stress on S_t, where S_t is that part of the bounding surface on which the stress is explicitly specified.

The work function E and the complementary work function E_c in inequalities [6] and [7] are defined as

$$E = \int_0^{II} \eta\,\mathrm{d}II$$

and

$$E_c = \int_0^{II_\tau} \frac{\mathrm{d}II}{4\eta}, \qquad [8a,b]$$

where η is the generalised Newtonian viscosity and II and II_τ are the second invariants of the rate-of-deformation and the stress tensors respectively. Furthermore, for the flow of an Ellis fluid, the work function E is not a homogeneous function and hence only bounds on the upper and lower bounds for the energy dissipation rate per unit volume are obtainable (Slattery 1972). When the Ellis parameter $\alpha \geqslant 1$,

$$2E \geqslant \mathrm{tr}\,(\boldsymbol{\tau} \cdot \nabla\mathbf{v}) \geqslant \frac{\alpha+1}{\alpha} E. \qquad [9]$$

For the free surface model, the energy dissipation rate is wholly within the unit cell as the cell does no work on the surroundings. The bounding surface S is the surface of the solid sphere and the free surface. On the former, the velocity is specified and hence $(S - S_v)$ is the free surface. For a trial velocity profile, $v_r^* = 0$ on the free surface. Using [4], it can be shown that

$$\int_{S-S_v} (\mathbf{v}^* - \mathbf{v}) \cdot ([\mathbf{T} - \rho\bar{\phi}\mathbf{I}] \cdot \mathbf{n})\,\mathrm{d}S = 0. \qquad [10]$$

Further, for a trial stress profile that satisfies $\tau_{r\theta} = 0$ on the free surface, we have, from [4a]

$$\int_{S-S_v} \mathbf{v} \cdot ([\mathbf{T}^* - \rho\bar{\phi}\mathbf{I}] \cdot \mathbf{n})\,\mathrm{d}S = 0. \qquad [11]$$

Combining [6], [7] and [9] to [11], the bounds on the upper and lower bounds for the energy dissipation rate $\mathscr{E}$ are given by

$$2\int_V E^*\,dV \geqslant \left[\mathscr{E} = \int_V \operatorname{tr}(\boldsymbol{\tau}\cdot\nabla\mathbf{v})\,dV\right]$$
$$\geqslant \frac{\alpha+1}{\alpha}\left[-\int_V E_c^*\,dV + \int_{S(r=1)} \mathbf{v}\cdot([\mathbf{T}^* - \rho\bar{\phi}\mathbf{I}]\cdot\mathbf{n})\,dS\right]. \qquad [12]$$

3. UPPER BOUND

Since the flow is ϕ independent, a dimensionless stream function ψ is defined such that

$$\frac{v_r}{V_0} = -\frac{1}{r^2\sin\theta}\frac{\partial\psi}{\partial\theta}, \quad \frac{v_\theta}{V_0} = \frac{1}{r\sin\theta}\frac{\partial\psi}{\partial r}. \qquad [13a,b]$$

A trial stream function profile is chosen of the form

$$\psi^* = \left(A_1r^2 + A_2r^\sigma + \frac{A_3}{r} + A_4r^4\right)(1-z^2). \qquad [14]$$

Using [3], [4], [13] and [14], we get,

$$A_1 + A_2 + A_3 + A_4 = -\tfrac{1}{2},$$
$$2A_1 + \sigma A_2 - A_3 + A_4 = -1,$$
$$r_\infty{}^3A_1 + r_\infty{}^{\sigma+1}A_2 + A_3 + r_\infty{}^5A_4 = 0,$$
$$(\sigma-1)(\sigma-2)r_\infty{}^{\sigma+1}A_2 + 6A_3 + 6A_4r_\infty{}^5 = 0. \qquad [15]$$

For $\sigma = 1$, [14] with the constants A_1 to A_4 given by [15] reduces to the stream function profile for Newtonian flow.

The constitutive equation for the Ellis fluid is

$$\boldsymbol{\tau} = \frac{2\eta_0}{1 + (S_0/\sqrt{2}\tau_{1/2})^{\alpha-1}}\mathbf{D}, \qquad [16]$$

where $S_0 = \sqrt{II_\tau}$, η_0 is the shear rate viscosity, $\tau_{1/2}$ is an Ellis model parameter and $\mathbf{D}$ is the rate-of-deformation tensor.

Using [8a] and [16], it can be shown that

$$2\int_V E^*\,dV = \frac{\eta_0(V_0/a)^2}{4}\int_V \bar{S}_0^{*2}\left[1 + \frac{2\alpha}{\alpha+1}(N_1\bar{S}_0^*)^{\alpha-1}\right]dV \qquad [17]$$
$$= \pi\eta_0V_0{}^2aJ_1/2, \qquad [18]$$

where

$$J_1 = \int_{-1}^{1}\int_{x_\infty}^{1} \bar{S}_0^{*2}\left[1 + \frac{2\alpha}{\alpha+1}(N_1\bar{S}_0^*)^{\alpha-1}\right]x^{-4}\,dx\,dz \qquad [19]$$

and

$$N_1 = (\eta_0V_0/\sqrt{2}a\tau_{1/2}),\ x = 1/r \text{ and } x_\infty = 1/r_\infty.$$

The quantity $\bar{S}_0^*$ is obtained as the solution of the equation

$$\frac{\bar{S}_0^{*2}}{4}[1 + (N_1\bar{S}_0^*)^{\alpha-1}]^2 = \overline{II}^*, \qquad [20]$$

where the dimensionless second invariant of the trial rate-of-deformation tensor, $\overline{II}^*$ is given by

$$\overline{II}^* = II^*(a/V_0)^2 = 6z^2\left[(2-\sigma)A_2x^{3-\sigma} + 3A_3x^4 - \frac{2A_4}{x}\right]^2 + \frac{(1-z^2)}{2}\left[(\sigma-1)(\sigma-2)A_2x^{3-\sigma} + 6A_3x^4 - \frac{6A_4}{x}\right]^2. \quad [21]$$

From a macroscopic energy balance,

$$V_0F_d = \mathscr{E} \quad [22]$$

where F_d is the drag force.

Equations [18] and [22] and the first of the inequalities in [12] combine to give

$$Y_E = \frac{C_dRe_E}{24} \leq \frac{J_1}{6}, \quad [23]$$

where C_d is the drag coefficient and Re_E is the Reynolds number $2aV_0\rho/\eta_0$. The upper bound Y_{UB} is obtained as the minimum of the R.H.S. of [23].

4. LOWER BOUND

For the Ellis fluid, the definition of E_c given by [8b] yields

$$E_c = \frac{\eta_0}{4}(V_0/a)^2\bar{S}_0^2\left[1 + \frac{2}{\alpha+1}(N_1\bar{S}_0)^{\alpha-1}\right]. \quad [24]$$

Trial extra stress profiles are chosen of the form,

$$\begin{aligned}
\tau^*_{rr} &= -(\eta_0V_0/a)(Cx^D + C'x^B + C''/x)z,\\
\tau^*_{\theta\theta} &= -(\eta_0V_0/a)(Ex^D + E'x^B + E''/x)z,\\
\tau^*_{\phi\phi} &= -(\eta_0V_0/a)(Fx^D + F'x^B + F''/x)z,\\
\tau^*_{r\theta} &= -(\eta_0V_0/a)(A'x^B + A''/x)(1-z^2)^{1/2}.
\end{aligned} \quad [25]$$

Since the pressure p is defined as

$$p = -\frac{1}{3}\text{tr}\,[\mathrm{T}] \quad [26]$$

and the elements of the extra stress tensor are given by

$$\tau_{ij} = T_{ij} - p\delta_{ij},$$

it is required that

$$\text{tr}\,[\tau] = 0. \quad [27]$$

Therefore, from [25],

$$\begin{aligned}
C + E + F &= 0,\\
C' + E' + F' &= 0,\\
C'' + E'' + F'' &= 0.
\end{aligned} \quad [28]$$

Substituting the trial extra stress profiles into the equation of motion and equating $[\partial^2(p+\rho\bar{\phi})^*/\partial x\partial z] = [\partial^2(p+\rho\bar{\phi})^*/\partial z\partial x]$, and using [28], it can be shown that

$$\begin{aligned} E &= F, \\ E' &= F', \\ E'' &= F'', \\ D &= 2, \\ A' &= -3F'/(B-1), \\ F'' &= 2A''/3. \end{aligned} \qquad [29]$$

Using the condition of zero shear stress on the free surface,

$$A'' = -A'x_\infty{}^{B+1} \qquad [30]$$

Equations [28] to [30] specify ten of the constants that appear in [25] in terms of F, F' and B. Using [24], we have

$$\int_V E_c^*\,\mathrm{d}V = (\pi\eta_0 V_0^2 a/2)J_2, \qquad [31]$$

where

$$J_2 = \int_{-1}^{1}\int_{x_\infty}^{1} \bar{S}_0^{*2}\left[1+\frac{2}{\alpha+1}(N_1\bar{S}_0^*)^{\alpha-1}\right]x^{-4}\,\mathrm{d}x\,\mathrm{d}z \qquad [32]$$

and from the trial extra stress profile [25],

$$\bar{S}_0^{*2} = 6(Fx^2+F'x^B+F''/x)^2z^2+\frac{(1-z^2)}{2}(A'x^B+A''/x)^2. \qquad [33]$$

From the equation of motion, the trial pressure profiles are obtained on integration of the θ-component as

$$\frac{(p+\rho\bar{\phi})^*}{(\eta_0 V_0/a)} = [-Fx^2+\{(3-B)A'-F'\}x^B+(4A''-F'')/x]z+c_0(x), \qquad [34]$$

where c_0 is some function of x.

Using [3], [25] and [28] through [30] and [34], the surface integral term in [12] becomes,

$$\int_{S(r=1)} \mathbf{v}\cdot([\mathbf{T}-\rho\bar{\phi}I]^*\cdot\mathbf{n})\,\mathrm{d}S = 4\pi\eta_0 V_0^2 aF. \qquad [35]$$

Combining [12], [22], [31] and [35],

$$V_0F_d = \mathscr{E} \geqslant \frac{\alpha+1}{\alpha}\pi\eta_0 V_0^2 a(4F-J_2/2). \qquad [36]$$

Inequality [36] is written in dimensionless form as

$$Y_E = \left(\frac{C_d Re_E}{24}\right) \geqslant \frac{\alpha+1}{6\alpha}(4F-J_2/2). \qquad [37]$$

The maximum of the R.H.S. of inequality [37] gives the lower bound Y_{LB} on Y_E.

5. RESULTS AND DISCUSSION

The upper bound Y_{UB} was obtained by minimising the R.H.S. of inequality [23]. From [15], and [19–21], it is seen that J_1 is a function of σ alone and hence a Fibonacci search (Mangasrian 1972) on σ yields the upper bound. For each value of σ in the search, values of A_1 to A_4 were evaluated by solving the system of equations [15]. The quantity $\bar{S}_0^*$ in the integral [19] was obtained from [20] and [21] by a Newton–Raphson interation. The lower bound Y_{LB} was evaluated by maximising the R.H.S. of inequality [37] using a Rosenbrock search (Rosenbrock & Storey 1966) on F, F' and B. The integrals J_1 and J_2 were evaluated by a two-dimensional Simpson's quadrature.

The upper and lower bounds on Y_E are plotted in figure 2 for $N_1 = 0{\cdot}15$ and for various values of α and E. It is seen that the bounds diverge with increasing values of α. This is due to the fact that Y_{UB} and Y_{LB} are bounds on the upper and lower bounds. However, in most non-Newtonian flow situations, the values of N_1 and α are small and thus the bounds are sufficiently close for practical purposes.

Certain limiting behaviour on the bounds are also observed. For $N_1 \to 0$, inequality [9] becomes

$$\int_V 2E\,\mathrm{d}V = \int_V \mathrm{tr}\,(\tau \cdot \nabla \mathbf{v})\,\mathrm{d}V \leq \frac{\alpha+1}{2\alpha} \int_V 2E\,\mathrm{d}V. \qquad [38]$$

Since the trial stream function and the stress functions are chosen in a form that reduce to the Newtonian profiles, the upper and lower bounds on $[\int 2E\,\mathrm{d}V]$ yield the energy dissipation rate. Thus, because of inequality [38], the upper bound on the energy dissipation rate yields the Newtonian value and the lower bound yields $(\alpha+1)/2\alpha$ times the Newtonian value. Further, when $N_1 \to 0$ and $\alpha \to 1$, both the bounds reduce to the Newtonian value given by Happel (1958).

When N_1 is non-zero and $\alpha \to 1$, [16] indicates Newtonian behaviour with a viscosity equal to $(\eta_0/2)$. Thus, the bounds reduce to half the value of Y for a Newtonian fluid.

The limiting case $N_1 \to \infty$, corresponds to the power law fluid behaviour. From [16] it can be shown that

$$\eta = K(2II)^{(n-1)/2} \text{ (power law)},$$

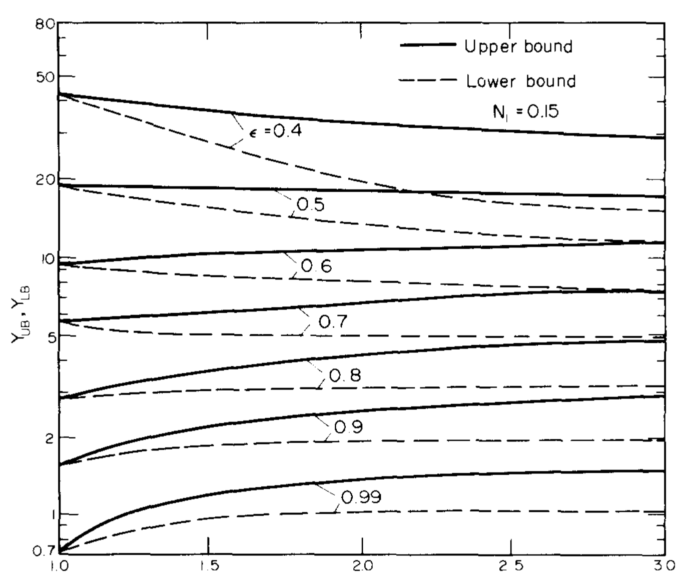

Figure 2. Upper and lower bounds on Y_E vs α for various values of ϵ ($N_1 = 0.15$).

where $K = \eta_0(2N_1^2)^{(1-\alpha)/2\alpha}(V_0/a)^{(1-\alpha)/\alpha}$ is the consistency index and $n = 1/\alpha$ is the flow behavior index.

The definition of the Reynolds number for the power law fluid given by

$$Re_p = (2a)^n V_0^{2-n}\rho/K \text{ yields, for large } N_1,$$

$$Y_E = Y_P(N_1/\sqrt{2})^{(1-\alpha)/\alpha}, \qquad [39]$$

where $Y_P = C_d Re_P/24$.

Equation [39] predicts a linear asymptotic behaviour for a plot of Y_E vs N_1 on log–log co-ordinates (figure 3). The asymptote has a slope of $(1-\alpha)/\alpha$ and passes through the point $(N_1 = \sqrt{2}, (Y_E)_B = (Y_P)_B)$, which yields the value of the bound on Y for a power law fluid with a flow behaviour index $n = 1/\alpha$. Thus, it is seen that the present analysis also yields the bounds on Y for the creeping flow of a power law fluid past an assemblage of spheres. These bounds are seen to be close despite the bound-on-bound approach used in obtaining the bounds on Y_E.

6. COMPARISON WITH EXPERIMENTAL DATA

It is profitable to represent the bounds on the drag as the bounds on $(f \cdot Re_E)$ where f is the Fanning friction factor $(a\Delta P/2\rho V_0^2 L)$. It can be shown that, for a packed bed of porosity ϵ and height L over which the pressure drop is ΔP,

$$f \cdot Re_E = 9Y_E(1-\epsilon). \qquad [40]$$

The experimental data on pressure drop for the flow of Ellis fluids in a packed bed was obtained by Sadowski (1965). Typical experimental values of Sadowski are compared in table 1 with the bounds on $(f \cdot Re_E)$ predicted from the present theory. A value of $\epsilon = 0.45$ was assumed since Sadowski did not report values for the voidage. It is seen from table 1 that the arithmetic mean of the bounds on the pressure drop for aqueous solutions of polyethylene glycol and polyvinyl alcohol agrees with the experimental values within 7% while, for solutions of Natrosol, the experimental values are much larger. This is understandable because Sadowski reported that his Natrosol solutions exhibited viscoelastic effects.

The results of the present investigation reveal that a combination of Happel's free surface

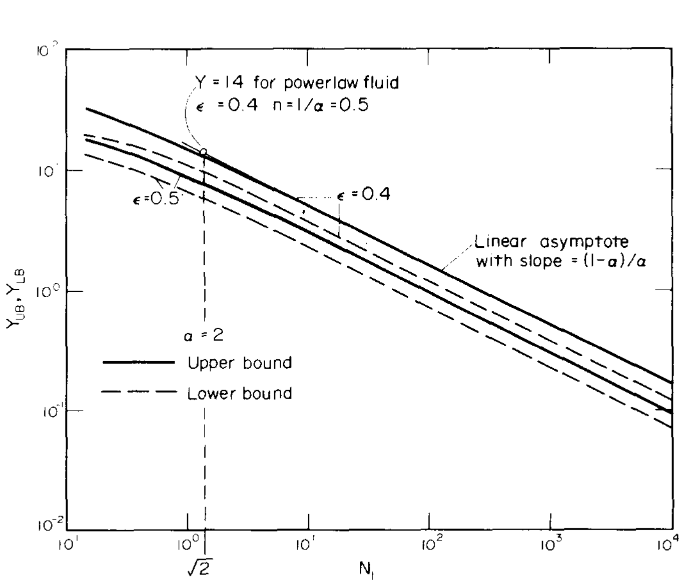

Figure 3. Asymptotic behaviour of the bounds for $N_1 \to \infty$ ($\alpha = 2$).

Table 1. Comparison of the theory with experimental data of Sadowski (1965)

Aqueous polymer solution	N_1	α	$(fRe_E)_{exp}$	$(fRe_E)_{UB}$	$(fRe_E)_{LB}$	$(fRe_E)_{mean}$
Polyethylene glycol (10% by weight)	0.1	1.651	133.2	137.3	108.8	123.0
Polyvinyl alcohol (6% by weight)	0.1	2.4	108.9	135.6	95.2	115.4
Natrosol (1% by weight)	3.0	1.64	110.8	50.0	40.0	45.0
Natrosol (1.85% by weight)	3.0	2.006	38.0	33.9	25.2	29.6

model and variational principles yield close bounds on the energy dissipation rate for the creeping flow of an Ellis fluid and that the drag can be predicted with reasonable accuracy for purely viscous systems using the arithmetic average of the bounds. The present analysis also forms a first step towards studying non-Newtonian flow in complicated geometries.

REFERENCES

Adachi, K., Yoshioka, N. & Yamamoto, K. 1973 On non-Newtonian flow past a sphere. *Chem. Engng Sci.* **28**, 2033–2043.

El-Kaissy, M. M. & Homsy, G. M. 1973 A theoretical study of pressure drop and transport in packed beds at intermediate Reynolds numbers. *IEC Fundamentals* **12**, 82–90.

Happel, J. 1958 Viscous flow in multiparticle systems. Slow motion of fluids relative to beds of spherical particles. *A.I.Ch.E. Jl* **4**, 197–201.

Happel, J. & Brenner, H. 1965 *Low Reynolds Number Hydrodynamics*. Prentice-Hall, New York.

Hopke, S. W. & Slattery, J. C. 1970 Upper and lower bounds on the drag coefficient of a sphere in an Ellis model fluid. *A.I.Ch.E. Jl* **16**, 224–229.

Kuwabara, S. 1959 The forces experienced by randomly distributed parallel circular cylinders or spheres in a viscous flow of small Reynolds numbers. *J. Phys. Soc. Japan* **14**, 527–532.

Le Clair, B. P. & Hamielec, A. E. 1968 Viscous flow through particle assemblages at intermediate Reynolds numbers. *IEC Fundamentals* **7**, 542–549.

Mangasrian, O. L. 1972 Techniques of optimization. *Trans. ASME, J. Engng. Ind.* Ser. B, **94**, 365–372.

Mohan, V. & Venkateswarlu, D. 1974 Lower bound on the drag offered to a Newtonian fluid sphere placed in a flowing Ellis fluid. *J. Chem. Engng. Japan.* **7**, 243–247.

Rosenbrock, H. H. & Storey, C. 1966 *Computational Techniques for Chemical Engineers.* Pergamon Press, Oxford.

Sadowski, T. J. & Bird, R. B. 1965 Non-Newtonian flow through porous media—I. Theoretical. *Trans. Soc. Rheol.* **9**, 243–250.

Sadowski, T. J. 1965 Non-Newtonian flow through porous media—II. Experimental. *Trans. Soc. Rheol.* **9**, 251–271.

Savins, J. G. 1969 Non-Newtonian flow through porous media. *Ind. Engng Chem.* **61**, (10) 18–47.

Slattery, J. C. 1962 Approximations to the drag force on a sphere moving slowly through either an Ostwald-de Waele or a Sisko fluid. *A.I.Ch.E. Jl* **8**, 663–667.

Slattery, J. C. 1972 *Momentum, Energy and Mass Transfer in Continua.* McGraw-Hill, New York.

Tomita, Y. 1959 On the fundamental formula of non-Newtonian flow. *Bull. J. S. M. E.* **7**, 469–474.

Wallick, G. C., Savins, J. G. & Artenburn, D. R. 1962 Tomita solution for the motion of a sphere in a power-law fluid. *Physics Fluids* **5**, 367–368.

Wasserman, M. L. & Slattery, J. C. 1964 Upper and lower bounds on the drag coefficient of a sphere in a power law fluid. *A.I.Ch.E. Jl* **10**, 383–388.